

# Cyanidin-3-O-glucoside Inhibits the $\beta$ -catenin/MGMT Pathway by Upregulating miR-214-5p to Reverse Chemotherapy Resistance in Glioma Cells

**Yuan Zhou**

Hubei University of Chinese Medicine

**Li Chen**

Hubei University of Medicine

**Deping Ding**

Hubei University of Medicine

**Ziheng Li**

Hubei University of Chinese Medicine

**Li Cheng**

Hubei University of Chinese Medicine

**Qiuyun You** (✉ [qiuyunyou@outlook.com](mailto:qiuyunyou@outlook.com))

Hubei University of Chinese Medicine

**Shunbo Zhang**

Hubei University of Chinese Medicine

---

## Research Article

**Keywords:** glioma, temozolomide, cyanidin-3-O-glucoside, resistance, miR-214-5p

**Posted Date:** August 12th, 2021

**DOI:** <https://doi.org/10.21203/rs.3.rs-783551/v1>

**License:**  This work is licensed under a Creative Commons Attribution 4.0 International License.

[Read Full License](#)

---

# Abstract

Overcoming resistance to alkylating agents has important clinical significance in glioma. Cyanidin-3-O-glucoside (C3G) has a tumor-suppressive effect on tumor cells. However, whether it plays a role in temozolomide resistance in glioma is still unclear. We construct a TMZ-resistant glioma LN-18/TR cells, observe the effect of C3G on TMZ resistance in these cells, and explore the role of miR-214-5p in chemoresistance. Results show that  $\beta$ -catenin and MGMT were significantly upregulated in LN-18/TR cells. C3G upregulated miR-214-5p and enhanced the cytotoxic effect of temozolomide on LN-18/TR cells. C3G downregulated  $\beta$ -catenin and MGMT. The miR-214-5p mimic downregulated  $\beta$ -catenin and MGMT in LN-18/TR cells, whereas the miR-214-5p inhibitor had the opposite effect. The miR-214-5p inhibitor significantly blocked the cyanidin-3-O-glucoside-induced downregulation of  $\beta$ -catenin and MGMT. C3G or the miR-214-5p mimic enhanced temozolomide-induced apoptosis in LN-18/TR cells, whereas the miR-214-5p inhibitor blocked this effect. Further, C3G or miR-214-5p agomir combined with TMZ could significantly inhibit the growth of LN-18/TR tumors. Our research has discovered the potential signaling mechanism associated with C3G-mediated suppression of TMZ resistance in LN-18/TR cells through miR-214-5p, which can facilitate the treatment of MGMT-induced resistance in glioma cells.

## Introduction

Glioma originates from the inner constituent cells of the brain and is a primary tumor of the central nervous system<sup>1</sup>. The current treatment for glioma is comprehensive treatment based on surgery, radiotherapy, and chemotherapy<sup>2</sup>. Because glioma is located in the brain, surgery is difficult, and it is difficult for drugs to pass through the blood-brain barrier, which complicates treatment. This is especially true for high-grade glioma, which progresses quickly and has a poor prognosis, presenting a major challenge for clinical treatment<sup>3,4</sup>. Alkylating agents have mild side effects and overcome the limitations of traditional chemotherapeutic drugs that do not easily penetrate the blood-brain barrier. Therefore, they have become important drugs for the treatment of glioma, with temozolomide (TMZ) being the most representative<sup>5,6</sup>. However, as with other chemotherapeutics, patients often develop acquired resistance after treatment with alkylating agents<sup>5,6</sup>. Acquired drug resistance often leads to failed alkylating agent treatment, which is also one of the main causes of patient death. Therefore, overcoming the resistance to alkylating agents has important clinical significance for the treatment of glioma.

Cyanidin-3-O-glucoside (C3G) is an anthocyanin and a water-soluble flavonoid compound widely found in plants, and mainly in blueberries, black rice, and purple potatoes<sup>7,8</sup>. The molecular formula of C3G is  $C_{21}H_{21}O_{11}$ , and the molecular structure is shown in Fig. 1. Its basic structure contains two benzene rings and a large number of phenolic hydroxyl groups<sup>9</sup>. Because of the unique molecular structure of C3G, it has a strong antioxidant effect<sup>9</sup>. Previous studies have shown that C3G has anti-inflammatory, anti-tumor, and fat metabolism roles<sup>10</sup>. C3G has been confirmed to have a tumor-suppressive effect in breast cancer<sup>11</sup>, colon cancer<sup>11,12</sup>, osteosarcoma<sup>13</sup>, and other malignant tumors, highlighting the relatively high

development value of C3G. However, the effect of C3G on chemotherapy resistance in glioma is still unclear, and further research is needed.

In recent years, microRNA (miRNA) has been found to play an important role in the occurrence and development of malignant tumors. miRNAs are generally 20–25 nt in length and play physiological roles through the post-transcriptional regulation of mRNAs<sup>14</sup>. Many miRNAs cause mRNA degradation through specific base pairing with target mRNAs, ultimately affecting the expression of the encoded proteins<sup>15,16</sup>. Some miRNAs are abnormally expressed and play a role in the resistance of tumor cells to chemotherapeutics<sup>17–19</sup>. miR-214-5p has a tumor-suppressive effect in a variety of malignant tumors mediated by inhibiting tumor cell proliferation, migration, invasion, and other malignant biological behaviors<sup>20,21</sup>. However, whether miR-214-5p plays a role in TMZ resistance in glioma is still unclear. This study aimed to construct a TMZ-resistant glioma cell line, observe the effect of C3G on TMZ resistance in these cells, and explore the role of miR-214-5p in chemoresistance. This will provide theoretical support for the clinical treatment of glioma.

## Results

### **β-catenin and MGMT are upregulated in LN-18/TR cells.**

The TMZ-resistant glioma cell LN-18/TR had significantly enhanced resistance to TMZ (Fig. 2A and 2B). The resistance index of LN-18/TR cells to TMZ was 4.51. The expression of β-catenin and MGMT was significantly higher in LN-18/TR cells than in LN-18 cells (Fig. 2C and 2D).

### **C3G induces TMZ sensitization and upregulation of miR-214-5p in LN-18/TR cells.**

There was no significant difference between LN-18 cells and LN-18/TR cells with regard to the effect of C3G (5 ~ 150 μM) on proliferation. Lower concentrations of C3G (5–60 μM) had little effect on the proliferation of either LN-18 or LN-18/TR cells (Fig. 3A), whereas higher concentrations (90 ~ 120 μM) significantly reduced the proliferation ability of both LN-18 and LN-18/TR cells (Fig. 3A). TMZ combined with 30, 60, and 90 μM C3G had a greater inhibitory effect on LN-18/TR cell viability than TMZ alone (Fig. 3B and 3C). Additionally, treatment with 30, 60, and 90 μM C3G for 24, 48, and 72 h dose-dependently upregulated miR-214-5p in LN-18/TR cells (Fig. 3D).

### **CTNNB1 has miR-214-5p-binding sequences.**

The results of the miRcode analysis showed that *CTNNB1*, the gene encoding β-catenin, had a miR-214-5p-binding site, and the sequence of the site was relatively conserved among species (Fig. 4A). RNA22 v2

analysis revealed that *CTNNB1* and miR-214-5p had multiple potential interaction sites (Fig. 4B and Fig. S1).

## **C3G downregulates $\beta$ -catenin and MGMT in LN-18/TR cells through miR-214-5p.**

Treatment with 30, 60, and 90  $\mu$ M C3G decreased  $\beta$ -catenin and MGMT levels in LN-18/TR cells (Fig. 5A). Since C3G-induced miR-214-5p might target *CTNNB1*, we assessed the effect of miR-214-5p on the expression of  $\beta$ -catenin and MGMT. The miR-214-5p mimic increased miR-214-5p levels in LN-18/TR cells, whereas the miR-214-5p inhibitor decreased miR-214-5p levels (Fig. 5B and 5C). The miR-214-5p mimic decreased  $\beta$ -catenin and MGMT levels in LN-18/TR cells, whereas the miR-214-5p inhibitor increased their levels (Fig. 5D). To further verify the role of miR-214-5p in C3G-mediated  $\beta$ -catenin and MGMT downregulation, we assessed the effect of C3G on the expression of  $\beta$ -catenin and MGMT proteins in LN-18/TR cells transfected with a miR-214-5p inhibitor. The miR-214-5p inhibitor blocked the ability of 30, 60, and 90  $\mu$ M C3G to decrease  $\beta$ -catenin and MGMT levels in LN-18/TR cells (Fig. 5E).

## **C3G inhibits resistance to TMZ through miR-214-5p.**

TMZ could weakly induce apoptosis in LN-18/TR cells, although treatment with 30, 60, and 90  $\mu$ M C3G enhanced TMZ-induced apoptosis (Fig. 6A and 6B). Transfection of the miR-214-5p mimic also enhanced TMZ-induced apoptosis in LN-18/TR cells (Fig. 6A and 6B). To observe the role of miR-214-5p in C3G-enhanced TMZ-induced apoptosis in LN-18/TR cells, we transfected the miR-214-5p inhibitor into LN-18/TR cells and assessed apoptosis after treatment with C3G and TMZ. The results showed that the miR-214-5p inhibitor blocked the effect of C3G on TMZ-induced apoptosis in LN-18/TR cells (Fig. 7A and 7B).

## **C3G and miR-214-5p promote TMZ sensitivity in vivo.**

We further observed the effects of C3G and miR-214-5p on TMZ-resistant LN-18/TR xenografts. In vivo results showed that TMZ had no obvious growth inhibitory effect on LN-18/TR tumors (Fig. 8A, C and D). C3G or miR-214-5p agomir combined with TMZ could significantly inhibit the growth of LN-18/TR tumors (Fig. 8A, C and D). However, at the end of the experiment, the body weights of the mice in the TMZ group were significantly lower than those in the control group, whereas the body weights of the mice in the C3G combined with TMZ or miR-214-5p agomir combined with TMZ group were significantly lower than those in the TMZ group (Fig. 8B).

## **Discussion**

In this study, we successfully constructed a TMZ-resistant glioma cell line (LN-18/TR) through the intermittent administration of TMZ and a gradual increase in its concentration. The resistance index of

LN-18/TR cells to TMZ was 4.51. We found that levels of  $\beta$ -catenin and MGMT were significantly upregulated in LN-18/TR cells compared with those in the parental (non-resistant) cells.  $\beta$ -catenin is a functional protein encoded by *CTNNB1* that can form a protein complex with the adhesion protein cadherin to participate in cell adhesion<sup>22,23</sup>.  $\beta$ -catenin is also an important signaling molecule in the classic Wnt signaling pathway that participates in the regulation of cell proliferation, differentiation, and apoptosis<sup>24,25</sup>.  $\beta$ -catenin plays an important role in the resistance of various malignant tumors to chemotherapy drugs, immunosuppressants, and targeted drugs<sup>26-28</sup>. MGMT is a unique DNA repair protein found in bacteria and mammals that can repair DNA damage caused by alkylation<sup>29</sup>. Under normal circumstances, MGMT protects normal tissues from the damage of alkylating agents, whereas in tumor tissues, it increases resistance to alkylating chemotherapeutics<sup>30,31</sup>. Previous studies have shown that MGMT is a downstream target of Wnt/ $\beta$ -catenin and can mediate Wnt/ $\beta$ -catenin-induced TMZ resistance<sup>32</sup>. Bi et al. found that  $\beta$ -catenin can upregulate MGMT to maintain TMZ resistance in glioma cells, whereas cordycepin can inhibit the  $\beta$ -catenin/MGMT pathway to alleviate TMZ resistance<sup>33</sup>. These findings suggest that the resistance of the LN-18/TR cells to TMZ is related to  $\beta$ -catenin/MGMT signaling.

C3G, a flavonoid widely found in plants, has been proven to exert a tumor-suppressive effect in malignant tumors. Our study found that C3G can sensitize LN-18/TR cells to TMZ. We also showed that C3G can upregulate miR-214-5p in LN-18/TR cells. Bioinformatics analysis showed that *CTNNB1* (the gene encoding  $\beta$ -catenin) and miR-214-5p have multiple potential interaction sites, indicating that *CTNNB1* could be a target of miR-214-5p. Therefore, we speculate that C3G might downregulate  $\beta$ -catenin through miR-214-5p, thereby sensitizing LN-18/TR cells to TMZ.

For further verification, we analyzed the molecular mechanism underlying the relationship among C3G, miR-214-5p,  $\beta$ -catenin, and MGMT. We found that C3G decreased  $\beta$ -catenin and MGMT in LN-18/TR cells. A miR-214-5p mimic and miR-214-5p inhibitor exerted negative and positive regulatory effects, respectively, on the expression of  $\beta$ -catenin and MGMT in LN-18/TR cells. In addition, a miR-214-5p inhibitor blocked the C3G-induced downregulation of  $\beta$ -catenin and MGMT in LN-18/TR cells. These results suggest that C3G targets  $\beta$ -catenin through miR-214-5p, thereby inhibiting the expression of MGMT. We then assessed the effect of C3G and miR-214-5p on TMZ-induced apoptosis in LN-18/TR cells. Both C3G and the miR-214-5p mimic enhanced TMZ-induced apoptosis in LN-18/TR cells. In contrast, the miR-214-5p inhibitor blocked the effect of C3G on TMZ-induced apoptosis in LN-18/TR cells. Therefore, C3G enhances TMZ-induced apoptosis in LN-18/TR cells through miR-214-5p. In vivo results showed that C3G or miR-214-5p agomir could enhance the response of LN-18/TR xenograft tumors to TMZ. However, C3G or miR-214-5p agomir combined with TMZ caused severe weight loss in nude mice with xenograft tumors. It is suggested that the toxic and side effects of the two might be relatively strong, and corresponding chemical modification or preparation methods need to be improved. Based on these results, we hypothesize that C3G might upregulate miR-214-5p and inhibit  $\beta$ -catenin, thereby inhibiting the expression of MGMT, which leads to TMZ sensitization in LN-18/TR cells. Our research has discovered the potential signaling mechanism associated with C3G-mediated suppression of TMZ resistance in LN-

18/TR cells through miR-214-5p, which can facilitate the treatment of MGMT-induced resistance in glioma cells.

In conclusion, our study confirmed that C3G has a TMZ-chemosensitization effect in glioma cells, which is related to the upregulation of miR-214-5p. miR-214-5p downregulates  $\beta$ -catenin, potentially via direct binding to *CTTNB1*, which downregulates MGMT and ultimately sensitizes cells to TMZ. Therefore, C3G might be a potential novel therapeutic drug for TMZ-resistant gliomas.

## Materials And Methods

### Construction of the TMZ-resistant glioma cell line LN-18/TR and cell culture.

LN-18 cells were purchased from Culture Collection of the Chinese Academy of Science (China). LN-18 cells were cultured in DMEM (high glucose) medium (Invitrogen, Carlsbad, CA, USA) containing 15% fetal bovine serum (Gibco-BRL, Grand Island, NY, USA), 50 U penicillin, and 50  $\mu$ g streptomycin (HyClone, Logan, UT, USA). To create the LN-18 resistant cell line (LN-18/TR), LN-18 cells were cultured in DMEM complete medium with increasing concentrations of TMZ (Sigma-Aldrich, St. Louis, MO, USA; 80–2560  $\mu$ M; drug resistance index 4.51). All cells were cultured in a cell incubator at 37°C, with 5% carbon dioxide, and 95% air.

### MTT analysis.

Cells were diluted to a concentration of  $6 \times 10^4$  cells/mL and seeded in a 96-well plate at 100  $\mu$ L/well. After drug (TMZ, C3G, or TMZ+C3G) treatment, the cells were treated with MTT (Solarbio, China) according to the manufacturer's protocol. Briefly, 100  $\mu$ L DMSO was added to each well and after shaking for 5 s, the absorbance was measured at 450 nm.

### Western blotting.

After drug (C3G, miR-214-5p mimic, or miR-214-5p inhibitor) treatment, cells were collected in a 1.5 mL centrifuge tube, and 0.12 mL radio-immunoprecipitation assay lysis buffer (Solarbio) was added to lyse the cells for 10 min. The lysates were centrifuged at  $11,000 \times g$  for 20 min at 4°C, and the supernatant (total protein) was transferred to a 0.5 mL tube. The total protein was quantified using a bicinchoninic acid protein quantification kit (Solarbio), and 10  $\mu$ L protein samples (3.5 mg/mL) were prepared in the loading buffer. Samples (total protein) were separated on a 10% SDS-PAGE gel. The separated protein was transferred from the gel to a polyvinylidene difluoride (PVDF) membrane (Absin, China). The PVDF membrane was blocked with 5% skimmed milk for 3 h and then incubated with primary antibodies against beta ( $\beta$ )-catenin (1:1000), O-6-methylguanine-DNA methyltransferase (MGMT) (1:1000), and  $\beta$ -actin (1:3000) (Cell Signaling Technology, Danvers, MA, USA) overnight at 4°C. The PVDF membrane was

washed three times with tris-buffered saline with 0.1% Tween 20 (TBST) and incubated with goat anti-rabbit IgG HRP-conjugated secondary antibody (Cell Signaling Technology) at 20°C for 1 h. The PVDF membrane was washed with TBST, and 200 µL of enhanced chemiluminescent solution was added dropwise for color development. Imaging was performed under a gel imager. ImageJ (1.48v) software was used to analyze the density of the protein bands.

## Immunofluorescence analysis.

Sterilized coverslips were placed in a six-well plate, and  $5 \times 10^5$  cells per well were added. Cells were cultured for an appropriate time and fixed with 4% paraformaldehyde (Beyotime Biotechnology, China). The wells were rinsed with PBS, and 1 mL 0.1% Triton X-100 (Sigma-Aldrich) was added to each well for 10 min. The wells were rinsed again with PBS, and goat serum (Tianhang, China) was added dropwise to the coverslips and incubated for 1 h. The serum was blotted with absorbent paper, and diluted  $\beta$ -catenin (1:100) or MGMT (1:50) antibodies were added dropwise onto the coverslip. Coverslips were incubated overnight at 4°C. Slides were washed with PBS, and diluted fluorescent secondary antibody (Invitrogen, Carlsbad, CA, USA) was added dropwise to the coverslip. Coverslips were incubated for 1 h, at which point they were washed with PBS and Prolong® Gold Antifade Reagent (Beyotime Biotechnology) with 4',6-diamidino-2-phenylindole (Solarbio) was added dropwise. Slides were incubated for 5 min in the dark and mounted overnight at room temperature. The next day, the slides were imaged using an ECLIPSE Ts2R-FL fluorescence microscope (Nikon, Japan).

## Real-time fluorescence quantitative polymerase chain reaction (RT-FqPCR).

Cells were collected in a 1.5-mL tube and the total RNA was extracted with a Trizol kit (Sigma-Aldrich) following the manufacturer's protocol. A reverse transcription kit (Qiagen, Duesseldorf, Germany) was used to reverse transcribe total RNA into cDNA. cDNA was amplified using miR-214-5p primers and SYBR Premix Ex Taq™ (Takara Bio Inc., Japan) on an ABI 7500 RT-FqPCR machine (Applied Biosystems, Foster City, CA, USA). The sequence of the miR-214-5p and U6 primers are as follows: miR-214-5p forward, 5'-ACACTCCAGCTGGGACAGCAGGCACAGAC-3'; miR-214-5p reverse, 5'-CTCAACT

GGTGTCGTGGA-3'; U6 forward, 5'-GCTTCGGCAGCACATATACTAAAAT-3'; U6 reverse, 5'-CGCTTCACGAATTTGCGTGTCAT-3'.

## Bioinformatics.

miRcode (<http://www.mircode.org/index.php/>) was used to predict the probability of miR-214-5p binding sites in *CTNNB1* and conservation of the binding sites among species. RNA22 v2

(<https://cm.jefferson.edu/>) was used to predict complementary binding sites in miR-214-5p and *CTNNB1*.

## Transfection.

LN-18/TR cells were seeded in a 10 cm dish at  $1 \times 10^6$  cells/dish. The following day, DMEM containing miR-214-5p mimic (50 nM; Thermo Fisher Scientific, Waltham, MA, USA) or miR-214-5p inhibitor (120 nM; Thermo Fisher Scientific) and the corresponding negative control (NC) were prepared. Transfection was performed following the manufacturer's instructions. Cells were cultured for 24 h, at which point the medium was replaced. After 24 h, cells were harvested for RT-FqPCR to verify the level of miR-214-5p.

## Flow cytometry.

After drug treatment, cells were collected in a 10 mL tube and resuspended in  $1 \times$  Binding Buffer (Solarbio) at a concentration of  $1 \times 10^6$  cells/mL. The cells were mixed quickly and thoroughly. The cell suspension (100  $\mu$ L) was transferred to a flow tube. To this, fluorescein isothiocyanate Annexin V and propidium iodide (PI; Solarbio) were added according to the manufacturer's instructions and incubated for 20 min. Apoptosis was analyzed with an Accuri C6 Plus flow cytometer (BD Bioscience, San Jose, CA, USA).

## Animal experiments

The experiment was approved by the ethics committee of Hubei University of Chinese Medicine. Animal experiments were conducted in accordance with the Declaration of Helsinki and the ARRIVE guidelines. LN-18/TR cells were inoculated into the right armpit of BALB/c nude mice (HFK Bioscience CO., LTD, China) at  $5 \times 10^6$  per mouse. When tumors grew to approximately 100–150 mm<sup>3</sup>, animals were divided into groups as follows, with six animals in each group: control, TMZ (20 mg/kg/d ip), C3G (10 mg/kg/d ip) + TMZ (20 mg/kg/d ip), miR -214-5p agomir (1 mg/kg/3d iv; Thermo Fisher Scientific) + TMZ group (20 mg/kg/d ip). C3G or miR-214-5p agomir treatment was performed 4 h before TMZ administration. The experiment was carried out for 26 days, and the tumor long diameter, short diameter, and nude mouse body weight were recorded three times per week. At the end of the experiment, all nude mice were euthanized. Euthanized mice were anesthetized with isoflurane, and the tumor was stripped and weighed. Tumor volume was calculated as follows: tumor volume (mm<sup>3</sup>) = long diameter  $\times$  short diameter<sup>2</sup> / 2.

## Statistical analyses

GraphPad Prism 8.0 software for Windows was used to analyze the data. All results are shown as means  $\pm$  standard deviations. Comparisons between two groups were performed by a t-test; comparisons between multiple groups were performed by one-way analysis of variance followed by the least significant difference-*t* test for multiple comparisons.  $P < 0.05$  was considered significant.

## Date availability.

All data generated or analysed during this study are included in this published article.

## Declarations

## Acknowledgments and Funding

We would like to thank Editage ([www.editage.cn](http://www.editage.cn)) for English language editing. This work was supported by the National Natural Science Foundation of China (No. 81473560).

## Author contributions

Conception and design, Qiuyun You, Shunbo Zhang; Methodology, Yuan Zhou, Li Chen, Deping Ding; Acquisition of data, Yuan Zhou, Li Chen, Deping Ding, Ziheng Li, Li Cheng; Analysis and Interpretation of data, Qiuyun You, Shunbo Zhang, Yuan Zhou; Writing, Review and Editing, Qiuyun You, Shunbo Zhang, Yuan Zhou; Supervision, Qiuyun You.

## Competing interests

The authors do not have any possible conflicts of interest.

## Ethics declarations

We confirm the study was carried out in compliance with the ARRIVE guidelines. All methods were carried out in accordance with relevant guidelines and regulations.

## References

1. Cahill, D. & Turcan, S. *Origin of Gliomas. Semin. Neurol*, **38**, 5–10 (2018).
2. Karimi, P., Islami, F., Anandasabapathy, S., Freedman, N. D. & Kamangar, F. Advances in the molecular genetics of gliomas - implications for classification and therapy. *Nat. Rev. Clin. Oncol*, **14**, 434–452 (2017).

3. Ferris, S. P., Hofmann, J. W., Solomon, D. A. & Perry, A. Characterization of gliomas: from morphology to molecules. *Virchows Arch*, **471**, 257–269 (2017).
4. Davis, M. E. Epidemiology and Overview of Gliomas. *Semin. Oncol. Nurs*, **34**, 420–429 (2018).
5. Jiapaer, S., Furuta, T., Tanaka, S., Kitabayashi, T. & Nakada, M. Potential Strategies Overcoming the Temozolomide Resistance for Glioblastoma. *Neurol. Med Chir. (Tokyo)*, **58**, 405–421 (2018).
6. Lu, C. *et al.* DNA-methylation-mediated activating of lncRNA SNHG12 promotes temozolomide resistance in glioblastoma. *Mol. Cancer*, **19**, 28 (2020).
7. Wang, Z. *et al.* Cyanidin-3-O-glucoside attenuates endothelial cell dysfunction by modulating miR-204-5p/SIRT1-mediated inflammation and apoptosis., **46**, 803–812 (2020).
8. Kaewmool, C., Udomruk, S., Phitak, T., Pothacharoen, P. & Kongtawelert, P. Cyanidin-3-O-Glucoside Protects PC12 Cells Against Neuronal Apoptosis Mediated by LPS-Stimulated BV2 Microglial Activation. *Neurotox. Res*, **37**, 111–125 (2020).
9. Olivas-Aguirre, F. J. *et al.* Cyanidin-3-O-glucoside: Physical-Chemistry, Foodomics and Health Effects., **21**, 1264 (2016).
10. Guo, H. *et al.* Cyanidin 3-glucoside attenuates obesity-associated insulin resistance and hepatic steatosis in high-fat diet-fed and db/db mice via the transcription factor FoxO1. *J. Nutr. Biochem*, **23**, 349–360 (2012).
11. Yin, H. *et al.* Cyanidin-3-O-glucoside chloride acts synergistically with luteolin to inhibit the growth of colon and breast carcinoma cells. *Pharmazie*, **74**, 54–61 (2019).
12. Baster, Z. *et al.* Cyanidin-3-glucoside binds to talin and modulates colon cancer cell adhesions and 3D growth. *FASEB J*, **34**, 2227–2237 (2020).
13. Atashi, H. A. *et al.* Cyanidin 3-O-Glucoside Induces the Apoptosis in the Osteosarcoma Cells through Upregulation of the PPAR $\gamma$  and P21: An In Vitro Study. *Anticancer Agents Med. Chem*, **20**, 1087–1093 (2020).
14. Khan, A. Q. *et al.* Role of miRNA-Regulated Cancer Stem Cells in the Pathogenesis of Human Malignancies., **8**, 840 (2019).
15. Rupaimoole, R. & Slack, F. J. MicroRNA therapeutics: towards a new era for the management of cancer and other diseases. *Nat. Rev. Drug Discov*, **16**, 203–222 (2017).
16. Tiwari, A., Mukherjee, B. & Dixit, M. MicroRNA Key to Angiogenesis Regulation: MiRNA Biology and Therapy. *Curr. Cancer Drug Targets*, **18**, 266–277 (2018).
17. Ding, L. *et al.* MicroRNAs Involved in Carcinogenesis, Prognosis, Therapeutic Resistance and Applications in Human Triple-Negative Breast Cancer., **8**, 1492 (2019).
18. Mihanfar, A., Fattahi, A. & Nejabati, H. R. MicroRNA-mediated drug resistance in ovarian cancer. *J. Cell Physiol*, **234**, 3180–3191 (2019).
19. Zhang, W. C. microRNAs Tune Oxidative Stress in Cancer Therapeutic Tolerance and Resistance. *Int. J. Mol. Sci*, **20**, 6094 (2019).

20. Zheng, C., Guo, K., Chen, B., Wen, Y. & Xu, Y. miR-214-5p inhibits human prostate cancer proliferation and migration through regulating CRMP5. *Cancer Biomark*, **26**, 193–202 (2019).
21. Guo, M., Lin, B., Li, G., Lin, J. & Jiang, X. LncRNA TDRG1 promotes the proliferation, migration, and invasion of cervical cancer cells by sponging miR-214-5p to target SOX4. *J. Recept. Signal. Transduct. Res*, **40**, 281–293 (2020).
22. Terada, N., Karim, M. R., Izawa, T., Kuwamura, M. & Yamate, J. Immunolocalization of  $\beta$ -catenin, E-cadherin and N-cadherin in neonate and adult rat kidney. *J. Vet. Med. Sci*, **79**, 1785–1790 (2017).
23. Wang, T., Wang, R., Cleary, R. A., Gannon, O. J. & Tang, D. D. Recruitment of  $\beta$ -catenin to N-cadherin is necessary for smooth muscle contraction. *J Biol Chem*, **290**, 8913–8924 (2015).
24. Valenta, T., Hausmann, G. & Basler, K. The many faces and functions of  $\beta$ -catenin. *EMBO. J*, **31**, 2714–2736 (2012).
25. Katoh, M. Multi-layered prevention and treatment of chronic inflammation, organ fibrosis and cancer associated with canonical WNT/ $\beta$ -catenin signaling activation (Review). *Int. J. Mol. Med*, **42**, 713–725 (2018).
26. de Ruiz, M. *et al.*  $\beta$ -Catenin Activation Promotes Immune Escape and Resistance to Anti-PD-1 Therapy in Hepatocellular Carcinoma. *Cancer Discov*, **9**, 1124–1141 (2019).
27. Lu, Y. *et al.* lncRNA MIR100HG-derived miR-100 and miR-125b mediate cetuximab resistance via Wnt/ $\beta$ -catenin signaling. *Nat. Med*, **23**, 1331–1341 (2017).
28. Emons, G. *et al.* Chemoradiotherapy Resistance in Colorectal Cancer Cells is Mediated by Wnt/ $\beta$ -catenin Signaling. *Mol. Cancer Res*, **15**, 1481–1490 (2017).
29. Yi, G. Z. *et al.* Acquired temozolomide resistance in MGMT-deficient glioblastoma cells is associated with regulation of DNA repair by DHC2., **142**, 2352–2366 (2019).
30. Zhang, D. *et al.* The interplay between DNA repair and autophagy in cancer therapy. *Cancer Biol. Ther*, **16**, 1005–1013 (2015).
31. Fahrer, J. *et al.* DNA repair by MGMT, but not AAG, causes a threshold in alkylation-induced colorectal carcinogenesis., **36**, 1235–1244 (2015).
32. Wickström, M. *et al.* Wnt/ $\beta$ -catenin pathway regulates MGMT gene expression in cancer and inhibition of Wnt signalling prevents chemoresistance. *Nat. Commun*, **6**, 8904 (2015).
33. Bi, Y. *et al.*  $\beta$ -catenin contributes to cordycepin-induced MGMT inhibition and reduction of temozolomide resistance in glioma cells by increasing intracellular reactive oxygen species. *Cancer Lett*, **435**, 66–79 (2018).

## Figures

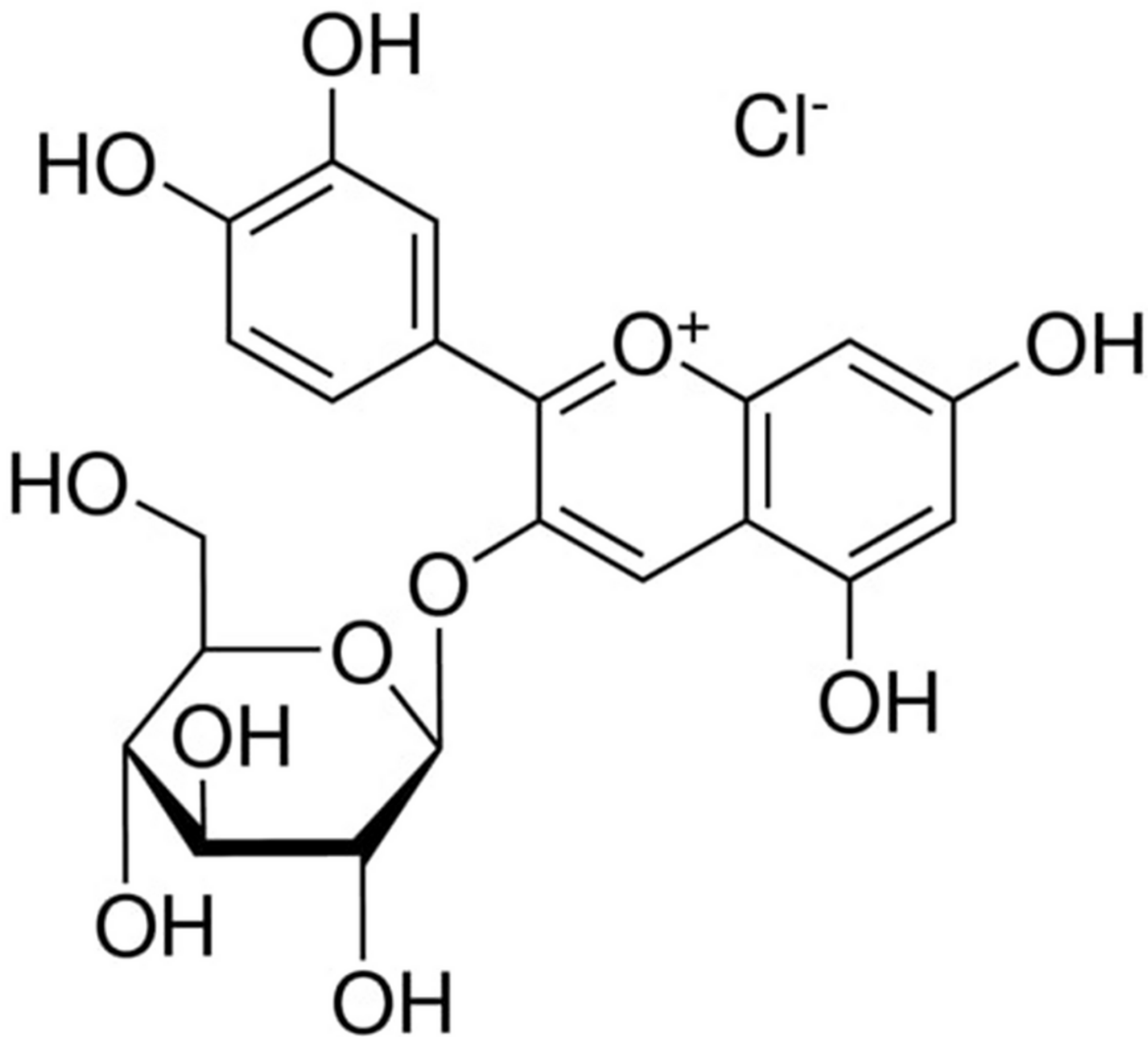
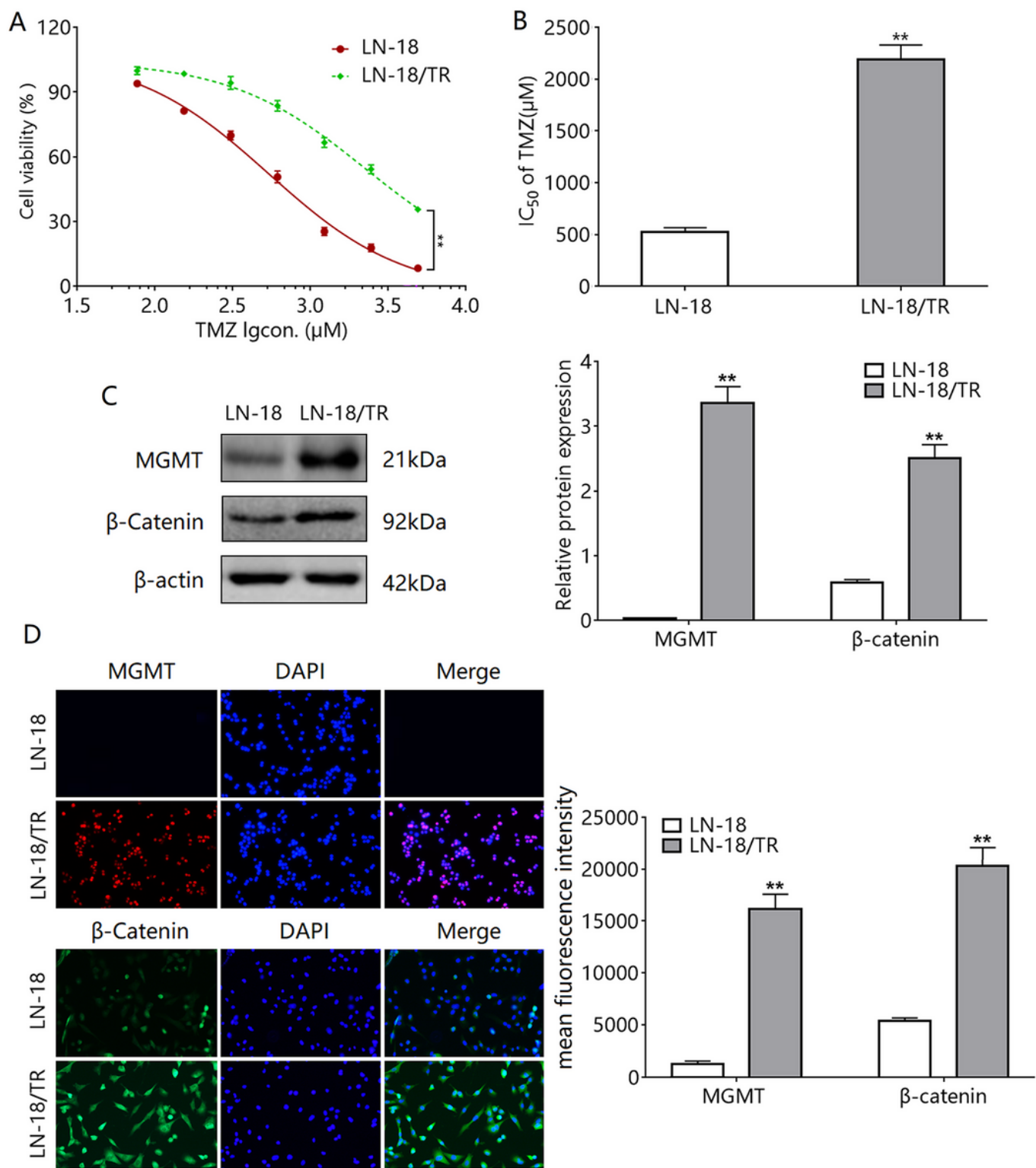


Figure 1

Molecular structure of cyanidin-3-O-glucoside (C3G).



**Figure 2**

Expression of  $\beta$ -catenin and MGMT in LN-18/TR cells. (A) LN-18 and LN-18/TR cells were treated with temozolomide (TMZ; 80, 160, 320, 640, 1280, 2560  $\mu$ M) for 72 h, and the cell proliferation inhibition rate was detected by the MTT method. (B) IC<sub>50</sub> of TMZ in cells. (C) Western blot was used to detect  $\beta$ -catenin and MGMT protein expression in cells. Images of full blots are available in supplementary information.

(D) Immunofluorescence was used to detect  $\beta$ -catenin and MGMT protein expression in LN-18 and LN-18/TR cells.  $**P < 0.01$  compared to LN-18 cells.

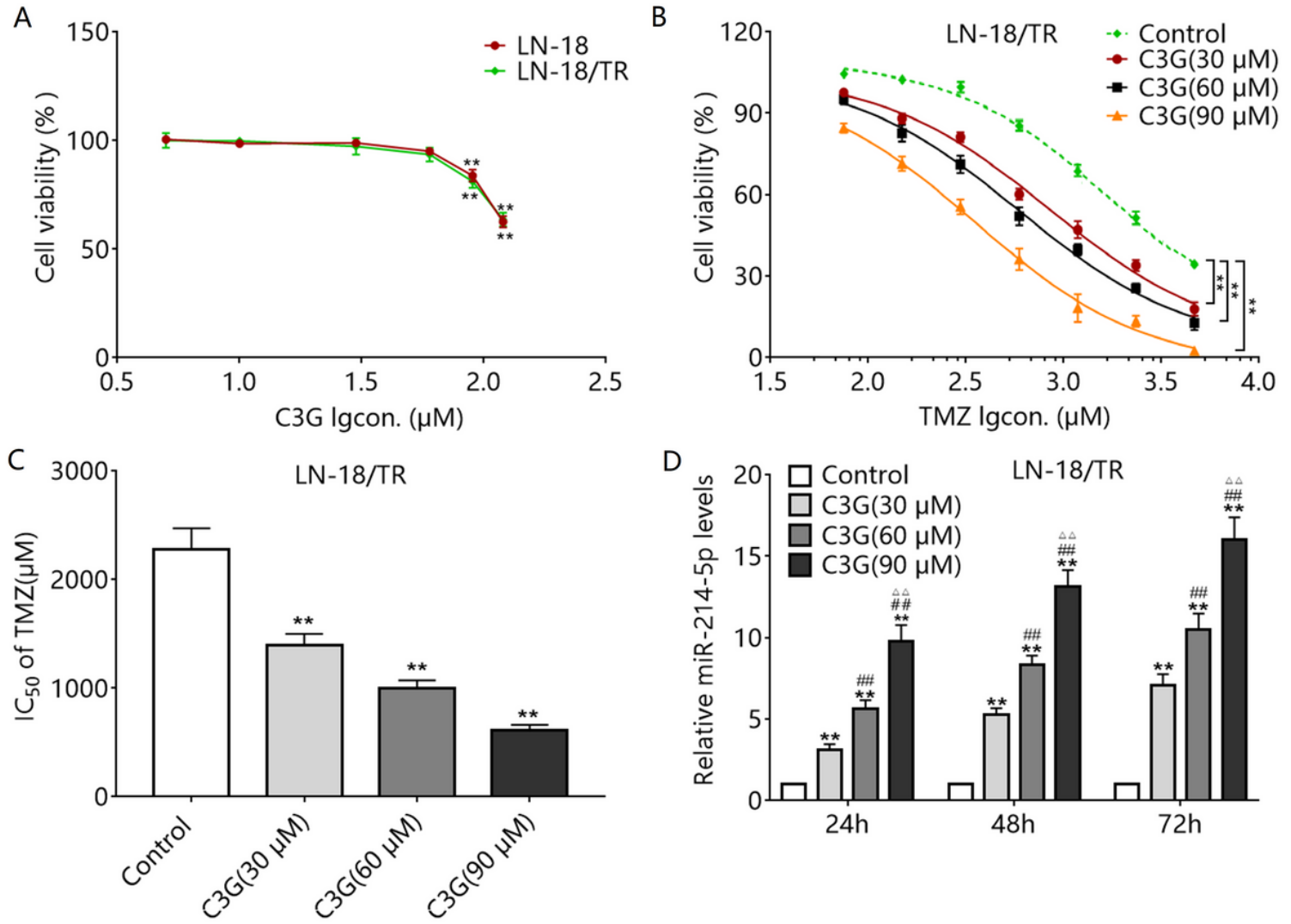


**Figure 3**

Cyanidin-3-O-glucoside (C3G) induces sensitization to temozolomide (TMZ) and the upregulation of miR-214-5p in LN-18/TR cells. (A) LN-18 and LN-18/TR cells were treated with C3G (5, 10, 30, 60, 90, 120  $\mu\text{M}$ ) for 72 h, and the cell proliferation inhibition rate was detected by the MTT method. (B) LN-18 and LN-18/TR cells were treated with C3G (30, 60, and 90  $\mu\text{M}$ ) combined with TMZ (80, 160, 320, 640, 1280, 2560  $\mu\text{M}$ ), and cell proliferation inhibition rate was detected by the MTT method. (C) The IC<sub>50</sub> of TMZ in LN-18/TR cells treated with 30, 60, and 90  $\mu\text{M}$  C3G. (D) LN-18/TR cells were treated with 30, 60, 90  $\mu\text{M}$  C3G, and the expression of miR-214-5p was assessed by RT-FqPCR.  $**P < 0.01$  compared to control.

A

ENSG00000168036.12 (CTNNB1) (coding)							
microRNA family	Seed position	Seed type	Transcript region	Repeat	Conservation		
					Primates	Mammals	Other vert.
miR-139-5p	chr3:41281188	7-mer-A1	3pUTR	no	89 %	83 %	46 %
miR-141/200a	chr3:41281536	7-mer-A1	3pUTR	no	89 %	78 %	23 %
miR-146ac/146b-5p	chr3:41281013	7-mer-A1	3pUTR	no	89 %	61 %	15 %
miR-150/5127	chr3:41281338	7-mer-m8	3pUTR	no	89 %	61 %	38 %
miR-214/761/3619-5p	chr3:41281868	7-mer-m8	3pUTR	no	100 %	74 %	62 %
miR-217	chr3:41281508	7-mer-A1	3pUTR	no	78 %	74 %	23 %

B

miR Name	transcript name	leftmost position of predicted target site	folding energy (in -Kcal/mol)	heteroduplex	p value
my_mir_nohead r_provided_1	my_seq_nohead r_provided_1	21906	-31.80	TATTTATGATCCTTTT TTTT TTTTAAATTC TTTAAGAGACAGGGTCTTGCTCTGTT-GCCCAGGCT :       :       : TGTCCTACTCGCTACAAGACGTGTCGTT CACATCTGTCCTGTGTACTGTTGAGACAGGTCGGTCCGG	1.23E-3
my_mir_nohead r_provided_1	my_seq_nohead r_provided_1	11348	-34.40	GTA CTGGACATAACTGTATATGCTATACTTTT TTTT TTTTGAGATGGCATCTCACTCTGTC-ACCCAGGCT :       :       : TGTCCTACTCGCTACAAGACGTGTCGTT CACATCTGTCCTGTGTACTGTTGAGACAGGTCGGTCCGG	1.49E-3
my_mir_nohead r_provided_1	my_seq_nohead r_provided_1	11864	-24.30	CTGAAATGTCCTTATGTGATGCATGCTTCATATCCAAAAATTAATCATTTCCTCACTGAAGCCATGCC :     :       :       : TGTCCTACTCGCTACAAGACGTGTCGTT CACATCTGTCCTGTGTACTGTTGAGACAGGTCGGTCCGG	5.31E-3

## Figure 4

Bioinformatics prediction of the binding of CTNNB1 to miR-214-5p. (A) miRcode predicted miR-214-5p-binding sites in CTNNB1 and the conservation of the binding sites among species. (B) RNA22 v2 predicted the representative sequence of the miR-214-5p-binding site in CTNNB1. CTNNB1: gene encoding the  $\beta$ -catenin protein.

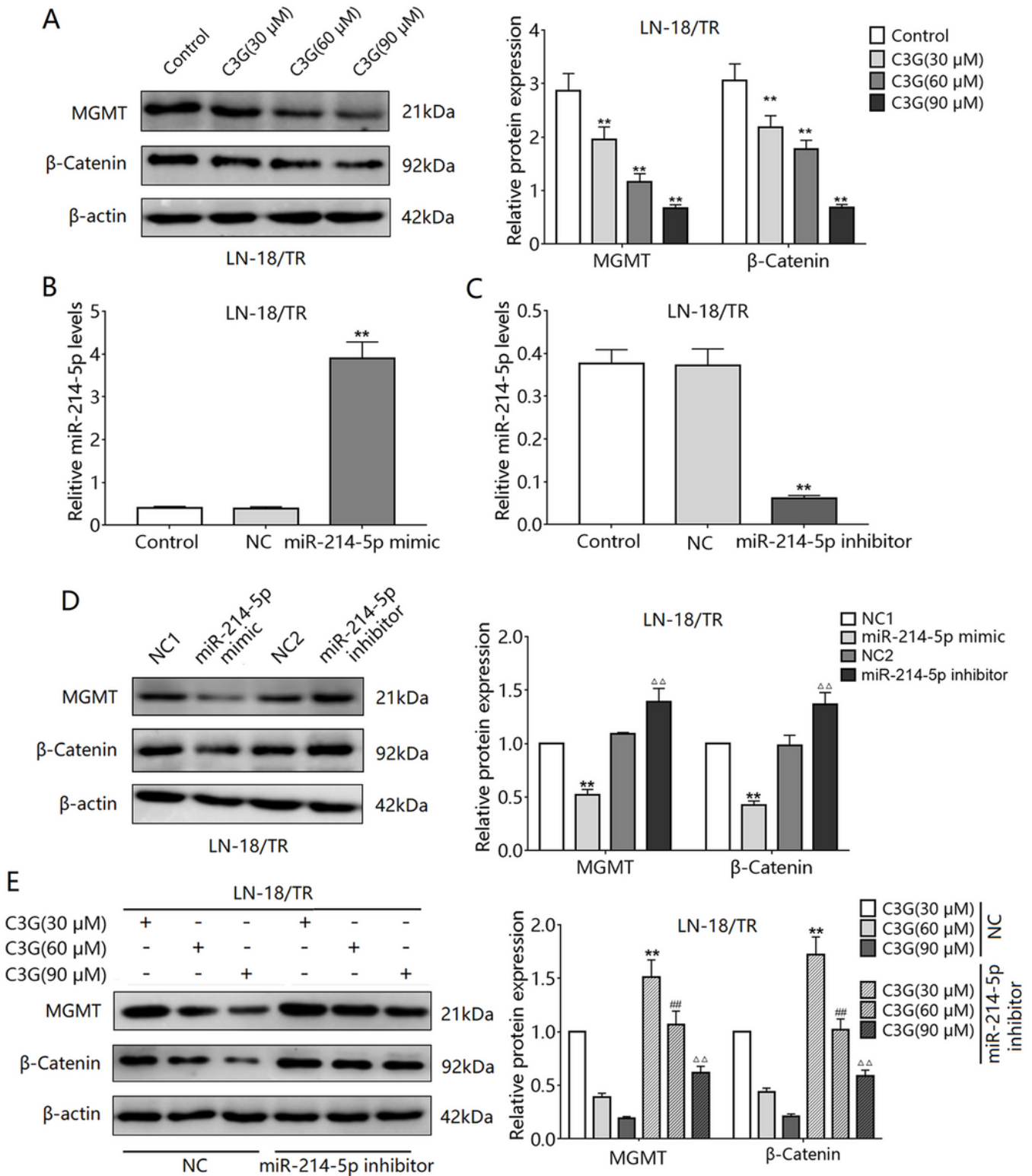


**Figure 5**

Cyanidin-3-O-glucoside (C3G) inhibits the  $\beta$ -catenin/MGMT signaling pathway through miR-214-5p. (A) LN-18/TR cells were treated with C3G (30, 60, and 90  $\mu$ M) for 48 h, and  $\beta$ -catenin and MGMT protein expression was detected in the cell protein extracts.  $**P < 0.01$  compared to the control. (B) RT-FqPCR was used to detect miR-214-5p levels in miR-214-5p mimic or negative control (NC) groups.  $**P < 0.01$  compared to NC. (C) RT-FqPCR was used to detect miR-214-5p levels in miR-214-5p inhibitor or NC

groups.  $**P < 0.01$  compared to NC. (D) Following promotion or inhibition of the miR-214-5p expression/activity in LN-18/TR cells,  $\beta$ -catenin and MGMT expression was detected in the cell protein extracts.  $**P < 0.01$  and  $\Delta\Delta P < 0.01$  compared to NC1 and NC2, respectively. (E) LN-18/TR cells were treated with 30, 60, or 90  $\mu\text{M}$  C3G for 48 h after transfection of NC or miR-214-5p mimic, and  $\beta$ -catenin and MGMT expression was detected in the cell protein extracts.  $**P < 0.01$ ,  $##P < 0.01$ ,  $\Delta\Delta P < 0.01$  compared to 30, 60, and 90  $\mu\text{M}$  C3G, respectively. Images of full blots are available in supplementary information.

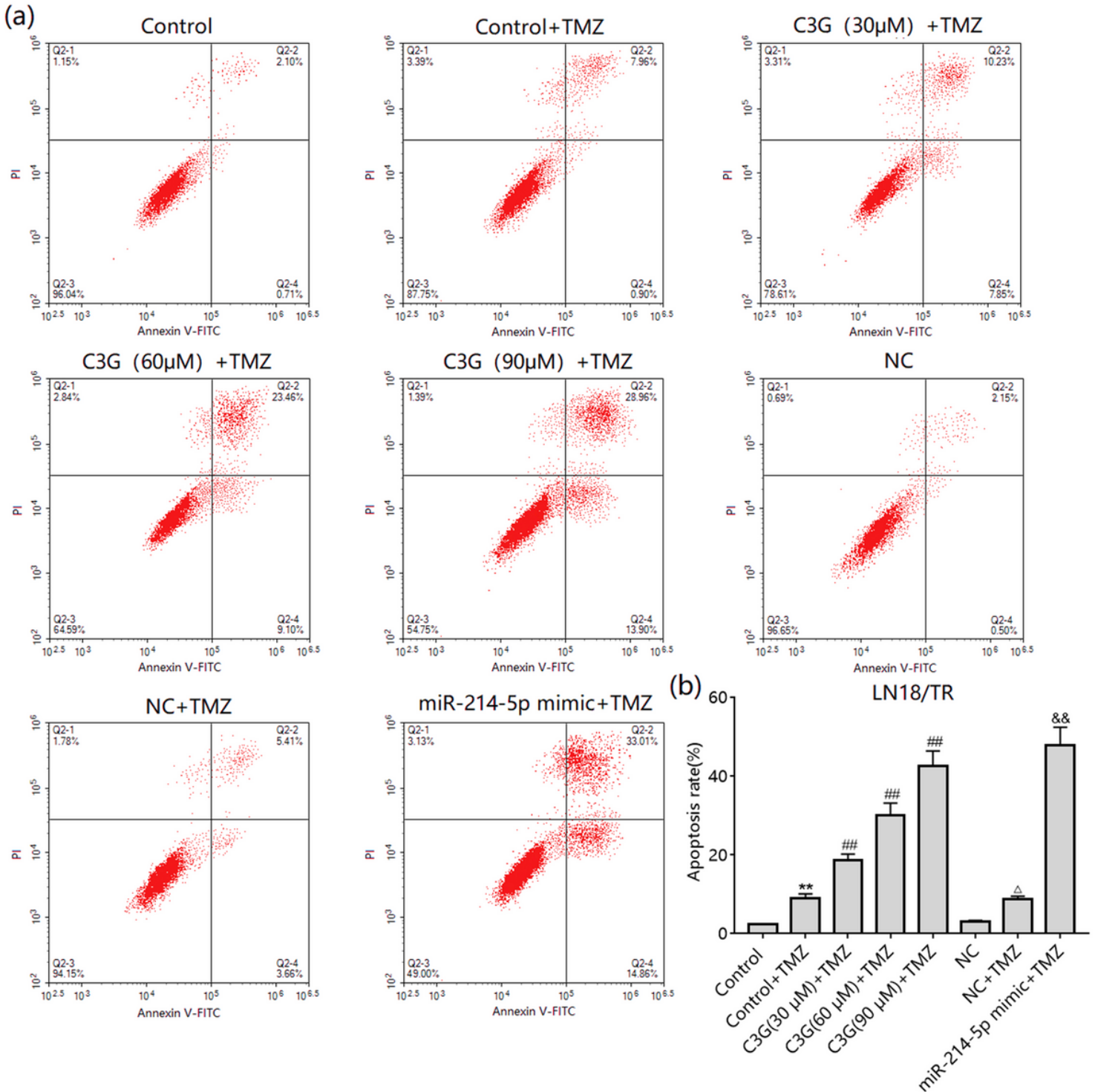
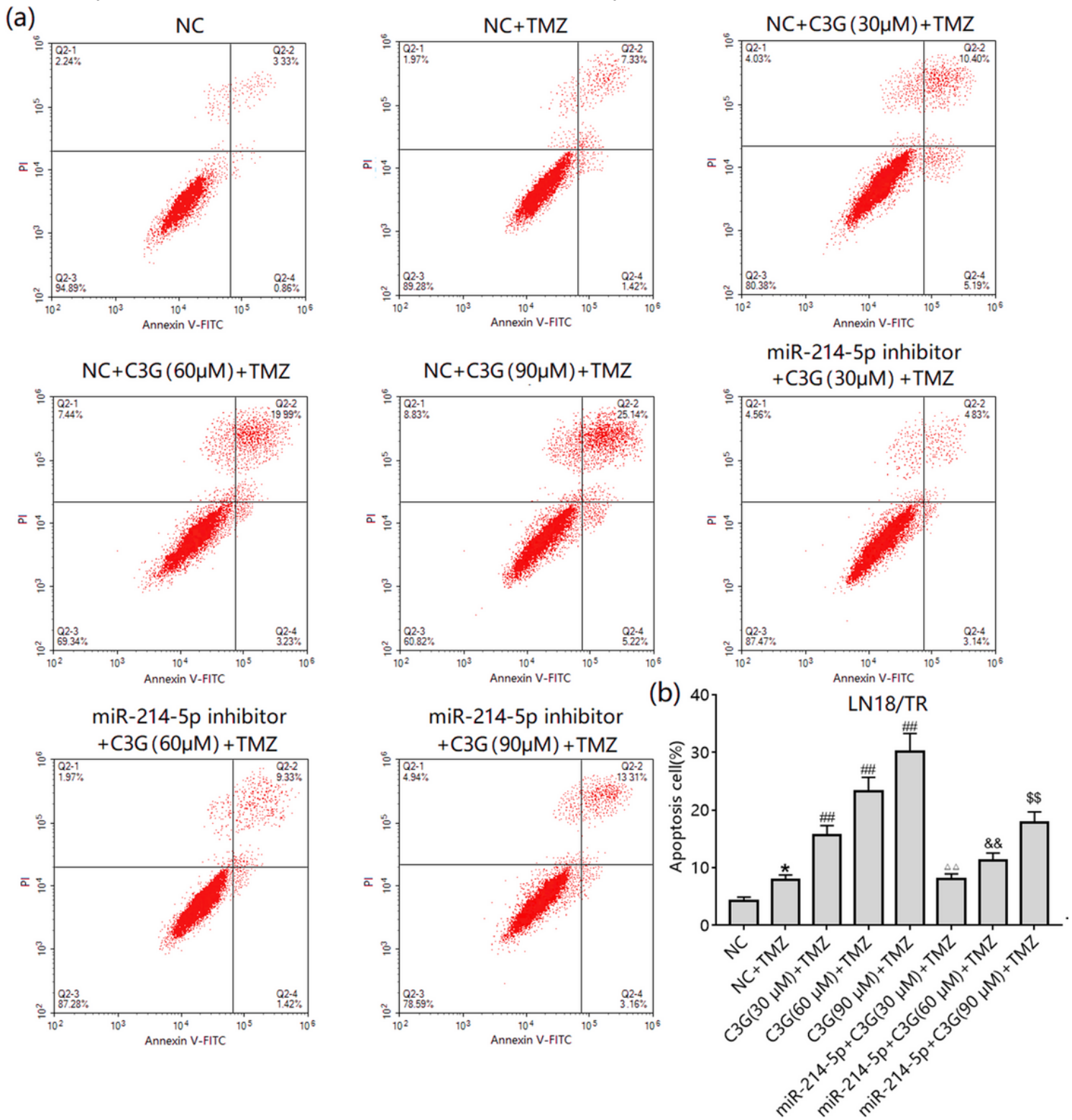


Figure 6

Cyanidin-3-O-glucoside (C3G) and miR-214-5p can enhance temozolomide (TMZ)-induced apoptosis in LN-18/TR cells. (A) LN-18/TR cells were treated with 1000  $\mu$ M TMZ alone or TMZ plus 30, 60, or 90  $\mu$ M C3G, NC, or miR-214-5p mimic for 72 h. Flow cytometry was used to detect apoptosis after each treatment. (B) The total apoptosis rate after each treatment. \*\*P < 0.01 compared to the control; ##P < 0.01 compared to control + TMZ;  $\Delta$ P < 0.05; &&P < 0.01 compared to NC+TMZ.



**Figure 7**

Cyanidin-3-O-glucoside (C3G) enhances the sensitivity of LN-18/TR cells to temozolomide (TMZ) by upregulating miR-214-5p. (A) LN-18/TR cells transfected with NC or miR-214-5p inhibitor were treated with 1000  $\mu$ M TMZ or TMZ plus 30, 60, or 90  $\mu$ M C3G for 72 h. Flow cytometry was used to detect apoptosis after each treatment. (B) The total apoptosis rate after each treatment. \* $P < 0.05$  compared to the control; ## $P < 0.01$  compared to NC+TMZ;  $\Delta\Delta P < 0.01$  compared to 30  $\mu$ M C3G+TMZ; && $P < 0.01$  compared to 60  $\mu$ M C3G+TMZ; \$\$\$ $P < 0.01$  compared to 90  $\mu$ M C3G+TMZ.

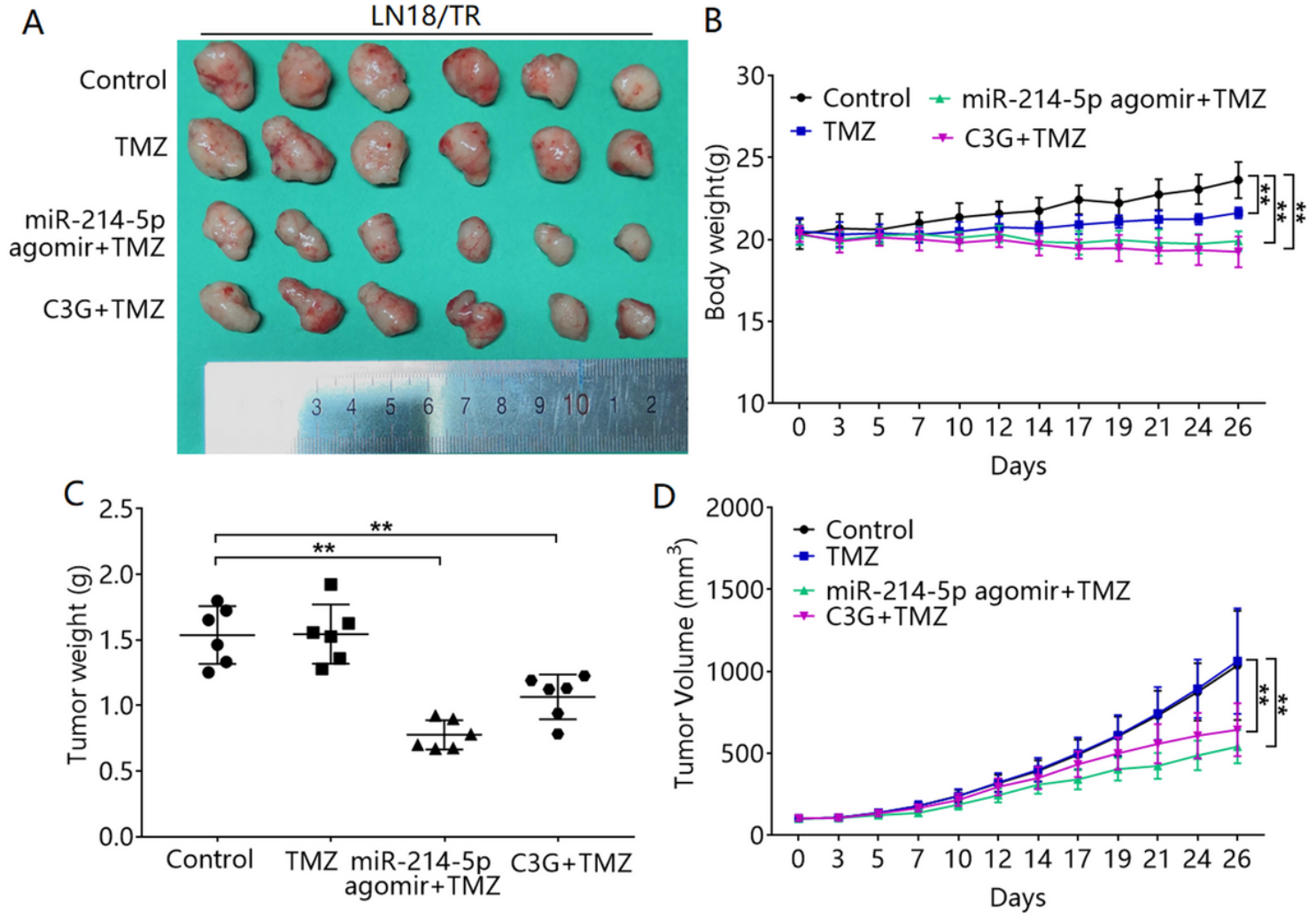


**Figure 8**

Cyanidin-3-O-glucoside (C3G) and miR-214-5p promote temozolomide (TMZ) sensitivity in vivo. (A) Control, TMZ, C3G+TMZ, miR-214-5p agomir+TMZ group tumor photos. (B) Changes in body weights of animals in each group. Compared with control, \*\* $P < 0.01$ . Compared with TMZ, ## $P < 0.01$ . (C) Tumor weights of each group of animals. \*\* $P < 0.01$ . (D) The tumor volume changes in each group of animals. Compared with control, \*\* $P < 0.01$ .

## Supplementary Files

This is a list of supplementary files associated with this preprint. Click to download.

- [FigureS1.pdf](#)
- [Westernblottingimage.pdf](#)